International Immunology, Vol. 32, No. 5, pp. 321–334
doi:10.1093/intimm/dxaa002
Advance Access publication 13 January 2020

Deficiency of TGR5 exacerbates immune-mediated cholestatic hepatic injury by stabilizing the β-catenin destruction complex

Jianhua Rao[1,2,3]*, Chao Yang[1,2,3]*, Shikun Yang[1,2,3,]*, Hao Lu[1,2,3], Yuanchang Hu[1,2,3], Ling Lu[1,2,3], Feng Cheng[1,2,3] and Xuehao Wang[1,2,3]

[1]Hepatobiliary Center, The First Affiliated Hospital of Nanjing Medical University, Nanjing 210029, China; [2]Key Laboratory of Liver Transplantation, Chinese Academy of Medical Sciences, Nanjing 210029, China; [3]NHC Key Laboratory of Living Donor Liver Transplantation, Nanjing 210029, China

Correspondence to: X. Wang; E-mail: wangxh@njmu.edu.cn or F. Cheng; E-mail: chengfeng@njmu.edu.cn

*These authors contributed equally to this work.

Received 11 March 2019, *editorial decision* 7 January 2020; *accepted* 10 January 2020

Abstract

Intrahepatic cholestasis induced by drug toxicity may cause cholestatic hepatic injury (CHI) leading to liver fibrosis and cirrhosis. The G protein-coupled bile acid receptor 1 (TGR5) is a membrane receptor with well-known roles in the regulation of glucose metabolism and energy homeostasis. However, the role and mechanism of TGR5 in the context of inflammation during CHI remains unclear. Wild-type (WT) and TGR5 knockout (TGR5$^{-/-}$) mice with CHI induced by bile duct ligation (BDL) were involved *in vivo*, and WT and TGR5$^{-/-}$ bone marrow-derived macrophages (BMDMs) were used *in vitro*. TGR5 deficiency significantly exacerbated BDL-induced liver injury, inflammatory responses and hepatic fibrosis compared with WT mice *in vivo*. TGR5$^{-/-}$ macrophages were more susceptible to lipopolysaccharide (LPS) stimulation than WT macrophages. TGR5 activation by its ligand suppressed LPS-induced pro-inflammatory responses in WT but not TGR5$^{-/-}$ BMDMs. Notably, expression of β-catenin was effectively inhibited by TGR5 deficiency. Furthermore, TGR5 directly interacted with Gsk3β to repress the interaction between Gsk3β and β-catenin, thus disrupting the β-catenin destruction complex. The pro-inflammatory nature of TGR5-knockout was almost abolished by lentivirus-mediated β-catenin overexpression in BMDMs. BMDM migration *in vitro* was accelerated under TGR5-deficient conditions or supernatant from LPS-stimulated TGR5$^{-/-}$ BMDMs. From a therapeutic perspective, TGR5$^{-/-}$ BMDM administration aggravated BDL-induced CHI, which was effectively rescued by β-catenin overexpression. Our findings reveal that TGR5 plays a crucial role as a novel regulator of immune-mediated CHI by destabilizing the β-catenin destruction complex, with therapeutic implications for the management of human CHI.

Keywords: CHI, Gsk3β, inflammation

Introduction

Bile duct obstruction is a major cause of chronic cholestasis, leading to progressive liver fibrosis and cirrhosis, regardless of the etiology (1). The accumulation of hydrophobic bile acids (BAs) is thought to induce chronic inflammation and hepatocyte apoptosis (2). Numerous studies have investigated the mechanisms involved in the development and resolution of cholestatic hepatic injury (CHI) at the cellular and molecular levels, and the immune response has been identified as one of the main mechanisms involved in the progression and repair of this liver pathology (3).

TGR5 is a novel bile acid receptor and a membrane-type G protein-coupled receptor (GPCR), consisting of 330 amino acids, including seven transmembrane domains (4, 5). TGR5 is widely expressed in various human organs, with the highest levels in the spleen and placenta, followed by the kidney, lung, liver, stomach, small intestine, and bone marrow. TGR5 is also expressed at lower levels in other tissues, such as the breast, uterine tissues, and skeletal muscles (6). Emerging evidence suggests that TGR5 regulates glucose homeostasis, increases energy expenditure in brown adipose tissue and contributes to BA homeostasis (7–9). TGR5 also exerts a potent anti-inflammatory effect, and its expression has been detected in macrophages, including Kupffer cells (KCs) in the liver (10). TGR5 activation

in macrophages has been reported to reduce phagocytic activity and pro-inflammatory cytokine production, suggesting an immune modulatory action of BAs through TGR5 (11–13). THP-1 cells over-expressing TGR5 suppressed cytokine production induced by lipopolysaccharide (LPS) challenge (5), and *in vivo* studies demonstrated that activation of TGR5 decreased LPS-induced inflammation in the liver (14) and in atherosclerotic plaques (13). However, the molecular mechanisms whereby TGR5 may regulate macrophage function and/or local inflammation responses in bile duct ligation (BDL)-induced CHI remain unknown.

β-catenin is the chief downstream effector of canonical Wnt signaling and has been shown to play an important role in liver development, metabolism and regeneration (15). In the absence of Wnt ligands, Ser/Thr residues in the N-terminus of β-catenin undergo constitutive phosphorylation by the cytoplasmic destruction complex containing adenomatous polyposis coli (APC), Axin, CK1α, and Gsk3β, which in turn facilitates ubiquitination of β-catenin by β-TrCP E3 ligase (16). β-catenin is rapidly accumulated in cytoplasm in response to Wnt signaling and subsequently enters the nucleus, where it interacts with T cell factor/lymphoid enhancer factor family members to regulate the transcription of target genes. The Wnt/β-catenin signaling pathway was also recently shown to play an essential role in pathological processes and chronic inflammation (17). The Wnt/β-catenin signaling pathway demonstrated cross-talk with nuclear factor-κB (NF-κB) signaling and Toll-like receptor (TLR)–mediated signaling (17–19). Innate immune receptor TLR4 activation causes a tissue inflammatory immune response and plays a key role in the pathogenesis of the disease, whereas inhibition of TLR4 exhibited significantly reduced inflammation in mice with CHI induced by BDL (20). In addition, previous studies have confirmed that TLR4 acted as a key molecule for controlling CHI *in vivo* (21, 22). Wnt/β-catenin signaling also inhibited endothelial and epithelial inflammatory responses by suppressing pro-inflammatory cytokines [tumor necrosis factor α (TNF-α) and interleukin (IL)-6] (23, 24), adhesion molecules (vascular cell adhesion molecule 1 and intercellular adhesion molecule 1) (25), and other inflammatory regulators (nitric oxide synthase type 2 and cyclooxygenase type 2) (18). Overall, these results suggest that aberrant expression of Wnt/β-catenin signals may contribute to inflammation (26, 27). It is therefore necessary to explore the emerging roles of Wnt/β-catenin signaling in the modulation of inflammatory responses. β-catenin signaling was also shown to be required for the control of innate and adaptive immunity during the inflammatory response (28). However, despite its essential immune modulatory functions, the physiological roles of β-catenin in macrophages during BDL-induced CHI are still unknown.

In this study, we identified a novel functional role and regulatory mechanism of TGR5 in the TLR4-mediated innate immune response during immune-mediated CHI. We demonstrated that TGR5 alleviated inflammatory responses by interacting with Gsk3β, subsequently disrupting the β-catenin destruction complex and promoting β-catenin signaling, which in turn activated PI3K/Akt and inhibited the TLR4/NF-κB pathway, eventually reducing BDL-induced CHI.

Methods

Patients

Liver tissues were obtained from 12 random consecutive patients, with clinically, biochemically, radiologically and histologically confirmed diagnoses of cholestatic liver disease, and from 12 age- and gender-matched healthy subjects. The inclusion criteria of the control group were patients with benign liver disease, including liver focal nodular hyperplasia, hepatic hemangioma and cysts. The baseline characteristics of CHI patients and controls are summarized in Supplementary Table S1. Informed consent was obtained from all participants, and the study was approved by the local ethics committee of Nanjing Medical University.

Animal experiments

Wild-type (WT) and TGR5 knockout (TGR5$^{-/-}$) C57BL/6 male mice (8 weeks old) (Model Animal Research Center of Nanjing University) were subjected to BDL, as described previously (29). Controls underwent a sham operation involving exposure of the common bile duct without ligation. Each experimental group included six mice. Mice were anesthetized by isoflurane and sacrificed at 1, 3 and 7 days after the BDL or sham operation. Serum was collected and the liver was removed. Animals received humane care in a temperature-controlled environment with a 12-h light–dark cycle. The animal protocol was approved by the Institutional Animal Care and Use Committee of Nanjing Medical University (protocol number IACUC-1702001).

Serum biochemistry and liver histopathology

Mice were sacrificed at 1, 3 and 7 days after BDL or sham surgery and liver tissues and blood were collected. Serum total BA (sTBA), total bilirubin (sTBIL), alanine aminotransferase (sALT) and aspartate transaminase (sAST) levels were measured using an AU5400 automated chemical analyzer (Olympus, Tokyo, Japan). Liver specimens were fixed in 4% paraformaldehyde, embedded in paraffin, sectioned at 4 μm, and stained with hematoxylin and eosin (H&E) and Masson's trichrome, according to standard protocols. The severity of liver injury was graded blindly using Suzuki's criteria on a scale of 0–4. The liver tissue collagen fiber was stained using Masson's trichrome, the results were analyzed by an image analyzer. The periphery and central region were selected from each slice, and the most visible field of collagen fibers was taken. Each field of view included the portal area, and the percentage of collagen fiber area was collagen fiber area/liver tissue area under a microscope at ×200.

Immunohistochemistry and immunofluorescence staining

Liver macrophages and neutrophils were detected using primary rabbit anti-mouse F4/80 (Cell Signaling Technology, Danvers, MA, USA) and rat anti-mouse Ly6G (Abcam, Cambridge, UK) monoclonal antibodies for immunofluorescence or immunohistochemistry staining. DAPI was used for nuclear counterstaining. Immunofluoresence staining was conducted using primary antibodies including rabbit anti-TGR5 (Novus, Littleton, CO, USA), mouse anti-Gsk3β (Abcam),

and rabbit anti-β-catenin (Cell Signaling Technology), and secondary antibodies including Alexa Fluor 488 goat anti-mouse IgG (Invitrogen, Life Technologies, Grand Island, NY, USA), and Alexa Fluor 594 goat anti-rabbit or anti-mouse IgG (Invitrogen). The cells were visualized using laser scanning confocal microscopy (Leica, Mannheim, Germany). The subcellular localization of β-catenin was determined by observing stained cells under a fluorescence microscope (Zeiss Axio Imager Z1, Carl Zeiss, Oberkochen, Germany). Positive cells were counted blindly in 10 high-power fields/section (×200). The stained tissue slices were scored by two different pathologists blinded to patients' clinical characteristics. The intensity of immunohistochemistry staining was scored as 0 (negative), 1 (weak), 2 (medium) and 3 (strong). The percentage of positive cells in the whole tissue slice was divided into five grades: 0 (≤10%), 1 (10–25%), 2 (26–50%), 3 (51–75%) and 4 (>75%). Intensity score and positive rate score were then multiplied to calculate the overall score.

Real-time polymerase chain reaction

Total cellular RNA was extracted from tissues and cultured cells using TRIzol reagent (Invitrogen, Carlsbad, CA, USA) and used to synthesize cDNA (Takara, Shiga, Japan). Quantitative PCR (qPCR) was performed using Fast Start Universal SYBR Green Master (Takara) with a 7900 Real-Time PCR System (Applied Biosystems, Foster City, CA, USA). All mRNA expression levels were corrected for expression of the reference genes encoding HPRT, GAPDH or β-actin in the same samples. All procedures were performed in triplicate. The primer sequences are given in Supplementary Table S2.

Western blotting

Tissues and cells were lysed using RIPA buffer supplemented with 1 mM PMSF and protease and phosphatase inhibitor (Beyotime, Shanghai, China). Lysates were incubated on ice and cleared by centrifugation at 12 000 × *g* for 10 min at 4°C. Proteins were separated by 10% denaturing polyacrylamide gel electrophoresis and transferred onto polyvinylidene difluoride membranes. After blocking in 5% nonfat milk, the membranes were exposed to specific primary antibodies against TGR5 (Abcam), β-catenin, p-β-catenin, p-Akt, p-Gsk3β, p-NF-κB p65, TLR4 and β-actin (Cell Signaling Technology) at a concentration of 1:1000. Membranes were then washed and exposed to peroxidase-conjugated secondary antibodies (Cell Signaling Technology). Immunoblots were imaged using a medical film processor (SRX-101A, Konica Minolta Medical & Graphic, Inc., NY, USA).

Co-immunoprecipitation

Cells were homogenized in cell lysis buffer (Beyotime) supplemented with 1 mM PMSF and complete protease inhibitor mixture (Beyotime). The homogenate was centrifuged at 12 000 × *g* for 8 min at 4°C. The supernatant was incubated with rabbit-anti-mouse TGR5 (Abcam) cross linked beads at 4°C overnight with rotation. Pretreatment of the beads and the immunoprecipitation step were carried out using a Pierce™ Cross link Magnetic IP Kit, according to the manufacturer's instruction. The associated protein was identified by western blot. Homogenates from co-culture cells were used as positive controls.

Measurement of TNF-α, IL-6 and IL-10 Levels

TNF-α, IL-6 and IL-10 levels in serum and cell culture medium were quantified using enzyme-linked immunosorbent assay (ELISA) kits (R&D, Minneapolis, MN, USA) according to the manufacturer's instructions. Three replicates were performed for each group.

Lentiviral vector construction, and isolation and transfection of murine bone marrow-derived macrophages

The pSin-β-catenin vector was constructed expressing β-catenin containing the EF2 promoter and puromycin gene. Bone marrow-derived macrophages (BMDMs) were generated as described previously (30). In brief, bone marrow cells were removed from the femurs and tibias of WT and TGR5$^{-/-}$ mice and cultured in DMEM supplemented with 10% fetal bovine serum (FBS) and 20% L929-conditioned medium. TGR5$^{-/-}$ BMDMs (1 × 10^6/well) were cultured for 7 days and then transfected with lentivirus expressing β-catenin or control vector. After 24–48 h, the cells were supplemented with 100 ng/ml LPS for an additional 24 h.

Cell migration assay

BMDMs isolated from WT and TGR5$^{-/-}$ mice were cultured and differentiated for 7 days, and then stimulated with LPS for 24 h. The supernatant was collected as conditioned medium and stored at −80°C. For cell migration assay, 1 × 10^4 WT BMDMs in 400 μl were seeded in the upper chambers of transwell units with 8-μm pore size polycarbonate filters (Millipore, Bedford, MA, USA) in serum-free medium, and 600 μl of the different conditioned media were added to the lower chambers. After incubation for 24 h, cells that did not migrate through the pores and remained in the upper chamber were removed by scraping the membrane with a cotton swab. The filters were also stained with 0.1% crystal violet for 30 min. The numbers of cells that migrated from the upper to the lower surface of the filter were counted and analyzed using a digital microscope system (Leica, Wetzlar, Germany).

Radiation schedules for animals and cell treatment

γ-Irradiation was administered using an X-ray source (RadSource RS2000 irradiator). Before irradiation, each mouse was anesthetized with isoflurane and subjected to whole-body irradiation at 5 Gy. Following irradiation, the mice were maintained at four to six animals per cage and supplied with standard laboratory chow and water *ad libitum*. WT BMDMs, TGR5$^{-/-}$ BMDMs and TGR5$^{-/-}$ BMDMs transfected with β-catenin-over-expressing or control vector were examined by cell membrane fluorescent labeling with PKH67 (Sigma–Aldrich, St. Louis, MO, USA) as previously described (31), according to the manufacturer's instructions. 5 × 10^6 cells were added to a polypropylene tube, centrifuged, and carefully aspirated to maximize removal of PBS. A2 staining solution of PKH67 was prepared by diluting 20 μl of 1 mM ethanolic dye solution in diluent C (both supplied with the kit) immediately before cell staining. Staining was

initiated by rapidly adding a 2× concentrated cell suspension, prepared by resuspending the cell pellet in 1 ml of diluent C, to the two dye solution. Staining was stopped after 3 min by adding an equal volume (2 ml) of FBS over a period of 1 min and subsequently an equal volume (4 ml) of complete medium containing 10% FBS. Cells were then centrifuged and washed three times with 10 ml of complete medium. All steps were performed at room temperature, and then cells were injected into the tail veins of mice in the respective groups, as described previously (32, 33). The mice were then subjected to a sham operation or BDL. The mice were sacrificed after 3 days for further experiments.

Statistical analysis

The results are presented as the mean ± standard deviation. Differences between two groups were used the Student's *t*-test. Multiple group comparisons were performed using one-way analysis of variance followed by Bonferroni's *post hoc* test. Comparisons between Kaplan–Meier curves were performed using log-rank tests. All analyses were performed using SPSS software (version 22.0). *P* values less than 0.05 (two-tailed) were considered statistically significant.

Results

TGR5 was up-regulated in liver tissues and KCs from patients with CHI and mice with BDL-induced CHI

To determine if TGR5 played a crucial role in CHI, we analyzed its expression in liver tissues from patients with CHI. TGR5 mRNA expression levels (9.50 ± 1.19 versus 1.15 ± 0.30; $P < 0.01$) were increased almost 10-fold in the livers of cholestatic patients compared with normal controls (Fig. 1A). Consistent with the mRNA expression levels, TGR5 protein levels were also significantly increased in cholestatic patients

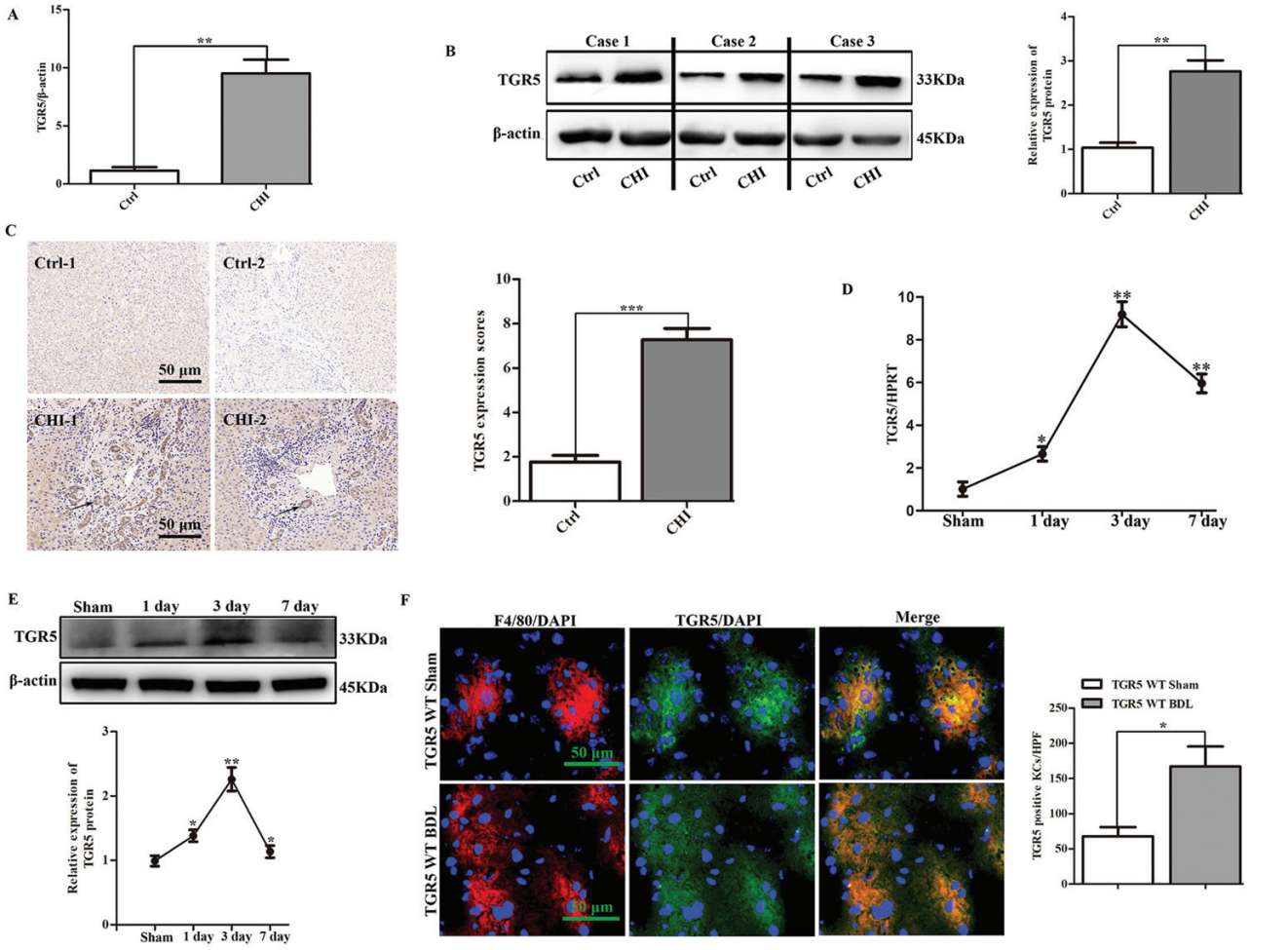

Fig. 1. TGR5 was up-regulated in liver tissues and KCs from patients with CHI and mice with BDL-induced CHI. (A) Gene expression level of TGR5 in human cholestatic livers ($n = 12$ for each group). (B) Western blotting analysis of TGR5 protein expression in human livers ($n = 3$). (C) Expression levels of TGR5 (black arrow) were compared between CHI patients and healthy subjects by immunohistochemistry ($n = 6$). Scale bars: 50 μm. (D) TGR5 gene expression levels were determined by qRT-PCR in WT mice 1, 3 and 7 days after sham operation or BDL ($n = 6$ for each group). (E) TGR5 protein expression levels were measured in WT mice at 1, 3 and 7 days after BDL with western blot ($n = 3$). (F) Dual-immunofluorescence staining of F4/80$^+$ macrophages (red) and TGR5 (green) in sections from WT mice following sham operation or at 3 days after BDL-induced liver cholestasis ($n = 6$). DAPI was used to visualize nuclei (blue). Scale bars: 50 μm. Statistical analysis was performed by Student's *t*-test. Results expressed as mean ± SD. $^*P < 0.05$, $^{**}P < 0.01$, $^{***}P < 0.001$.

compared with healthy subjects (Fig. 1B). These findings were confirmed by immunohistochemistry (Fig. 1C). WT mice were subjected to sham surgery or BDL, and TGR5 expression levels were assessed at 1, 3 and 7 days post-surgery. TGR5 transcription levels increased immediately and peaked at 3 days after BDL, then decreased gradually at 7 days (Fig. 1D). Similar results were observed for TGR5 protein levels during BDL-induced CHI (Fig. 1E). We also determined if TGR5 was activated in KCs in response to CHI *in vivo*. Dual immunofluorescence staining of F4/80 and TGR5 demonstrated that TGR5 co-localized in KCs, and TGR5-positive KCs were significantly increased in mice with BDL-induced CHI compared with sham-operation mice (Fig. 1F).

TGR5 deficiency exacerbated BDL-induced CHI in mice

We determined if TGR5 had a protective effect against BDL-induced CHI by analyzing serum and liver samples from age- and sex-matched WT and TGR5$^{-/-}$ mice harvested at 1, 3 and 7 days after sham surgery or BDL. sTBA, sTBIL and sALT levels in TGR5$^{-/-}$ mice were significantly increased compared with the levels in WT control mice at 1, 3 and 7 days after BDL (Fig. 2A–C). These results were consistent with those of liver pathological analysis and liver injury grading according to Suzuki's score (Fig. 2D). The liver fibrosis grade was significantly higher in the TGR5$^{-/-}$ compared with the WT group at 7 days after BDL (Fig. 2E). Notably, TGR5 deficiency significantly exacerbated liver injury and shortened survival in mice with BDL-induced CHI (Fig. 2F). Overall, these results support a protective role for TGR5 in CHI through its ability to attenuate liver injury and delay the progress of fibrosis.

TGR5 deficiency increased pro-inflammatory mediators and macrophage/neutrophil trafficking in BDL-induced CHI

Hepatic inflammation is known to contribute to cholestatic liver disease-related injury. We therefore analyzed the expression levels of inflammatory cytokines (TNF-α, IL-6 and IL-10) in the livers and serum of WT and TGR5$^{-/-}$ mice at 1,

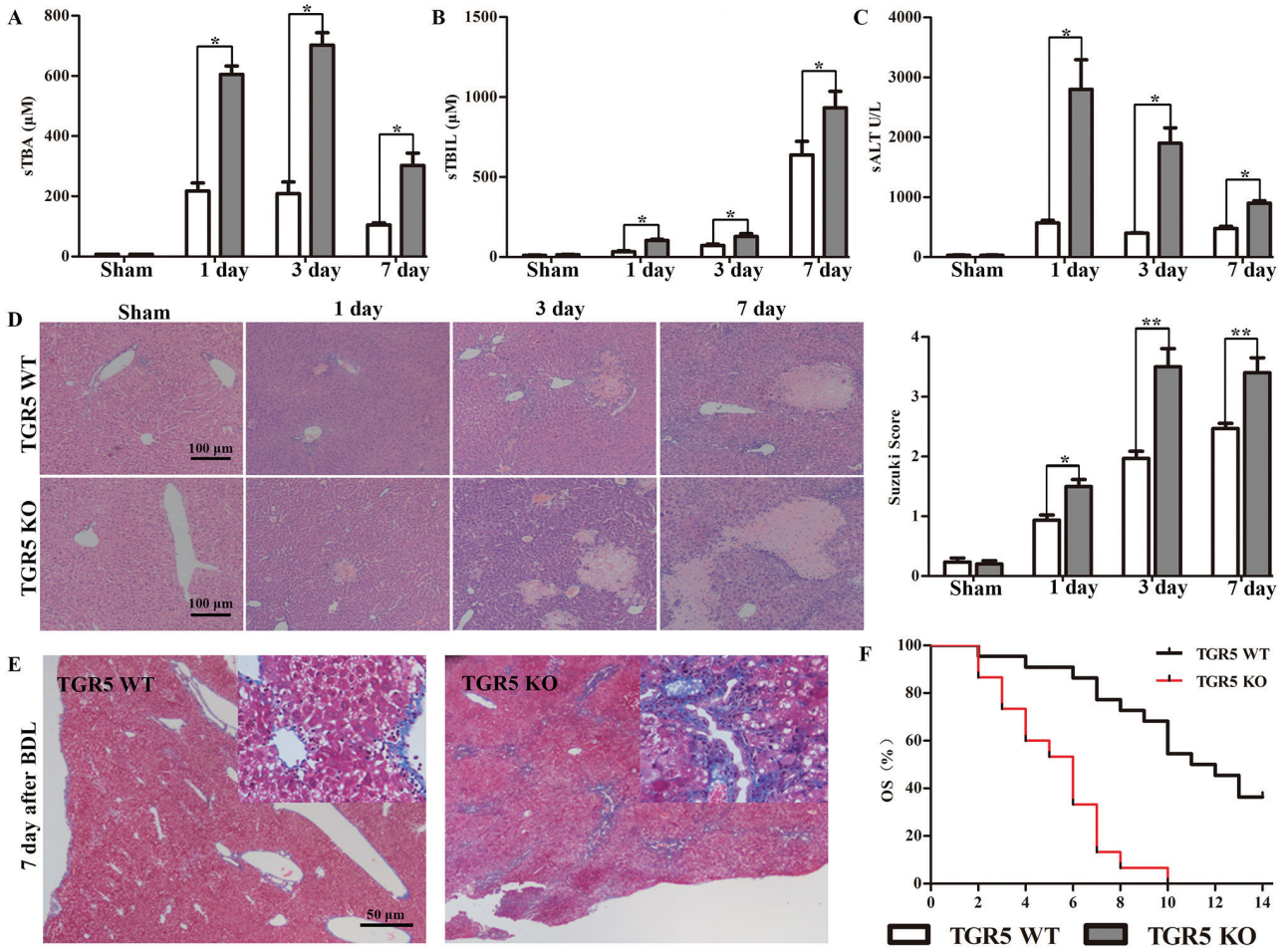

Fig. 2. TGR5 deficiency exacerbated BDL-induced CHI in mice. WT and TGR5$^{-/-}$ C57BL/6 mice were subjected to sham surgery or BDL, and liver tissues and serum were harvested at 1, 3 and 7 days after surgery. (A–C) sTBA, sTBIL and sALT levels in serum were determined (n = 6 for each group). (D) Representative histological staining (H&E) of cholestatic liver tissue (n = 6). Scale bars: 100 μm. Liver damage was evaluated by Suzuki's histological score. (E) Representative images of paraffin liver sections stained with Masson's trichrome (7 days after surgery) (n = 6). Scale bars: 50 μm. (F) Kaplan–Meier plots revealed an association between TGR5 deficiency and shorter survival in BDL-induced CHI. Statistical analysis was performed by Student's t-test. Results expressed as mean ± SD. $^{*}P < 0.05$, $^{**}P < 0.01$.

3 and 7 days after BDL. TNF-α, IL-6 and IL-10 mRNA levels were determined with qRT-PCR. TGR5$^{-/-}$ livers had significantly higher levels of TNF-α and IL-6, but lower levels of IL-10 than WT livers (Fig. 3A). Similar results were found in terms of serum levels of TNF-α, IL-6 and IL-10 analyzed with ELISA (Fig. 3B). We also analyzed macrophage and neutrophil accumulation in BDL-induced cholestatic livers by immunohistochemistry staining. There was no difference between the WT and TGR5$^{-/-}$ sham operation groups, but numbers of F4/80^{+} macrophages and Ly6G^{+} neutrophils were

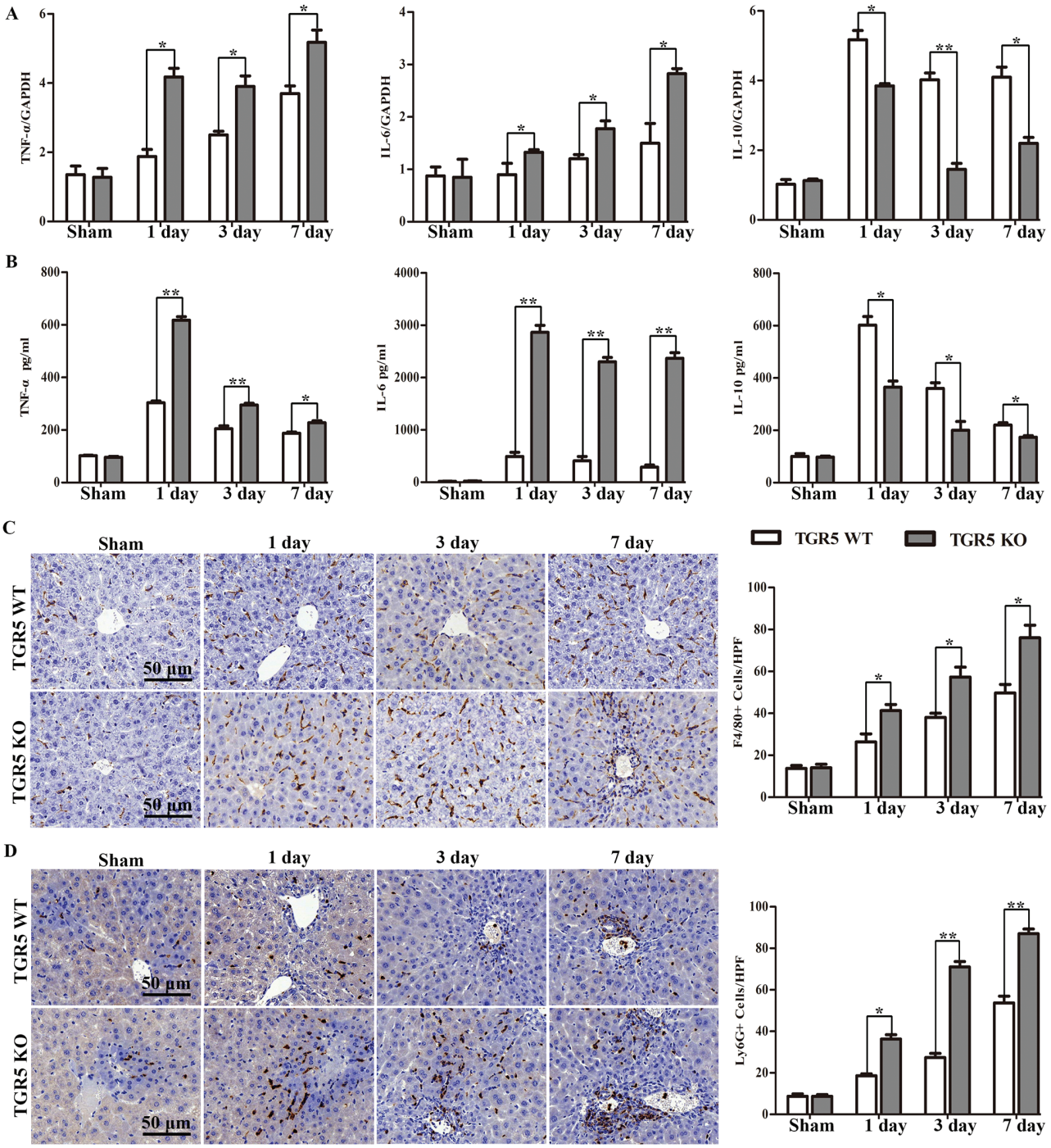

Fig. 3. TGR5 deficiency increased pro-inflammatory mediators and macrophage/neutrophil trafficking in BDL-induced CHI. WT and TGR5$^{-/-}$ mice were subjected to BDL or sham operation. (A) TNF-α, IL-6 and IL-10 mRNA levels were detected with qRT-PCR ($n = 6$ for each group) and (B) serum cytokine levels were measured with ELISA ($n = 6$). (C and D) Macrophage and neutrophil infiltration were analyzed by immunohistological staining with antibodies against F4/80 and Ly6G ($n = 6$), respectively. F4/80^{+} and Ly6G^{+} cells were quantitated by counting the numbers of positive cells/area. Scale bars: 50 μm. Statistical analysis was performed by Student's *t*-test. Results expressed as mean ± SD. $^{*}P < 0.05$, $^{**}P < 0.01$.

significantly higher in the livers of TGR5$^{-/-}$ BDL compared with WT BDL mice (Fig. 3C and D). These results suggest that the BDL-induced hepatic inflammatory response was significantly amplified in the absence of TGR5.

TGR5 activation inhibited TLR4-mediated pro-inflammatory responses in macrophages

We examined the effect of TGR5 on the inflammatory response *in vitro*. BMDMs isolated from WT and TGR5$^{-/-}$ mice were cultured and differentiated, and then stimulated with LPS for 24 h. The TGR5-specific agonist INT-777 was added 1 h before LPS stimulation. mRNA and protein levels of TNF-α, IL-6 and IL-10 were analyzed with qRT-PCR (Fig. 4A–C) and ELISA (Fig. 4D–F), respectively. TGR5$^{-/-}$ BMDMs expressed much higher TNF-α and IL-6 levels, but lower levels of IL-10 than WT BMDMs. INT-777 significantly reduced TNF-α and IL-6 expression levels and enhanced IL-10 expression in WT BMDMs, but had no effect in TGR5$^{-/-}$ BMDMs. These results indicated that TGR5 effectively inhibited pro-inflammatory cytokines and increased anti-inflammatory cytokines in macrophages.

Activation of intracellular signaling pathways by LPS/TLR4 was compared between the aforementioned groups. TLR4 and p-NF-κB p65 protein levels were markedly enhanced in TGR5$^{-/-}$ BMDMs after LPS treatment compared with WT BMDMs, as demonstrated by western blot (Fig. 4G). In contrast, LPS-phosphorylated Akt (Ser473) and p-Gsk3β were decreased in TGR5$^{-/-}$ BMDMs after LPS stimulation compared with the WT group (Fig. 4G). TGR5 activation by INT-777 pre-treatment followed by LPS stimulation further decreased TLR4 and p-NF-κB p65 protein expression levels in WT BMDMs, while INT-777 pre-treatment further increased p-Akt (Ser473) and p-Gsk3β in WT BMDMs (Fig. 4G).

TGR5 promoted β-catenin signaling pathway by disrupting the β-catenin destruction complex

We further explored the mechanisms whereby TGR5 inhibited the inflammatory response in macrophages by investigating the involvement of Wnt/β-catenin signaling pathways, which are known to be associated with the inflammatory response. We examined β-catenin mRNA and protein expression levels in cholestatic liver tissues from WT and TGR5$^{-/-}$ mice at 1, 3 and 7 days after BDL, by real-time PCR and western blotting, respectively. β-catenin mRNA expression was significantly lower in TGR5$^{-/-}$ mice with cholestatic liver compared with WT controls, and these results were confirmed by western blotting (Fig. 5A and B).

To determine if TGR5 specifically influenced β-catenin activation in macrophages, BMDMs isolated from WT and TGR5$^{-/-}$ mice were cultured and differentiated, and then treated with INT-777 for 1 h before LPS stimulation. β-catenin protein levels were significantly increased in WT BMDMs compared with TGR5$^{-/-}$ BMDMs at baseline. Following LPS stimulation, β-catenin protein levels were markedly elevated in WT BMDMs compared with TGR5$^{-/-}$ BMDMs. Moreover, INT-777 pretreatment further elevated β-catenin protein expression in response to LPS stimulation in WT BMDMs, but not in TGR5$^{-/-}$ BMDMs (Fig. 5C). Confocal microscopy showed that endogenous TGR5 could co-localize with endogenous Gsk3β in BMDMs (Fig. 5D). Moreover, co-immunoprecipitation assays indicated that TGR5 co-precipitated with endogenous Gsk3β in BMDMs (Fig. 5E). The interaction between TGR5 and Gsk3β led to destabilization of the β-catenin destruction complex, and p-β-catenin protein expression levels were significantly decreased in WT BMDMs compared with TGR5$^{-/-}$ BMDMs (Fig. 5F). Consistently, TGR5 increased the amount of cytoplasmic and nuclear β-catenin (Fig. 5G).

β-catenin signaling was essential for TGR5-mediated anti-inflammatory function in macrophages

We investigated the mechanisms responsible for the role of β-catenin in TGR5-mediated anti-inflammation by transfecting cultured BMDMs from WT and TGR5$^{-/-}$ mice with a β-catenin-over-expressing or control vector, followed by LPS stimulation. Lentivirus over-expressing β-catenin successfully up-regulated β-catenin protein expression in TGR5$^{-/-}$ BMDMs (Fig. 5H). Transfection of TGR5$^{-/-}$ BMDMs with the lentivirus vector containing the β-catenin DNA sequence markedly increased β-catenin expression in response to LPS stimulation, compared with control vector-transfected cells (Fig. 5H). As expected, β-catenin over-expression led to defective LPS-stimulated production of TNF-α and IL-6 in TGR5$^{-/-}$ macrophages, but increased expression of IL-10 compared with TGR5$^{-/-}$ BMDMs transfected with the control vector (Fig. 5I).

TGR5 deletion-induced chemokine expression and accelerated macrophage migration

TGR5$^{-/-}$ cholestatic liver tissues recruited more macrophages and neutrophils than WT liver tissues, as shown above, suggesting that the chemokine signaling network is crucial for macrophage functioning. We therefore analyzed the expression of the chemokine CXC chemokine ligand 10 (CXCL-10) and monocyte chemotactic protein 1 (MCP-1) in BDL-induced cholestatic liver tissues from WT and TGR5$^{-/-}$ mice. CXCL-10 and MCP-1 mRNA levels were significantly increased in TGR5$^{-/-}$ mice compared with WT mice at 1, 3 and 7 days after BDL (Fig.6A and B). Similar trends were observed in serum (data not shown). Given the increase in chemokines *in vivo*, we also investigated if TGR5 activation directly regulated chemokine expression *in vitro*. Following stimulation with LPS, TGR5$^{-/-}$ BMDMs produced higher expression levels of CXCL-10 and MCP-1 compared with WT BMDMs. INT-777-mediated TGR5 activation significantly attenuated the LPS-dependent increases in CXCL-10 and MCP-1 expression in WT BMDMs, but not TGR5$^{-/-}$ BMDMs (Fig. 6C and D). Furthermore, TGR5$^{-/-}$ macrophages over-expressing β-catenin decreased LPS-stimulated production of CXCL-10 and MCP-1 compared with TGR5$^{-/-}$ BMDMs transfected with the control vector (Fig. 6E and F).

Given the increase in chemokines *in vivo and vitro*, we next examined the effect of TGR5 on macrophage migration *in vitro*. First, BMDMs from WT and TGR5$^{-/-}$ mice were isolated and cultured for 7 days, and/or stimulated with LPS for 24 h. The supernatant was collected as conditioned medium. Supernatant collected from TGR5$^{-/-}$ BMDMs stimulated with LPS increased the ability of WT macrophages to migrate *in vitro* compared with supernatant from WT BMDMs stimulated

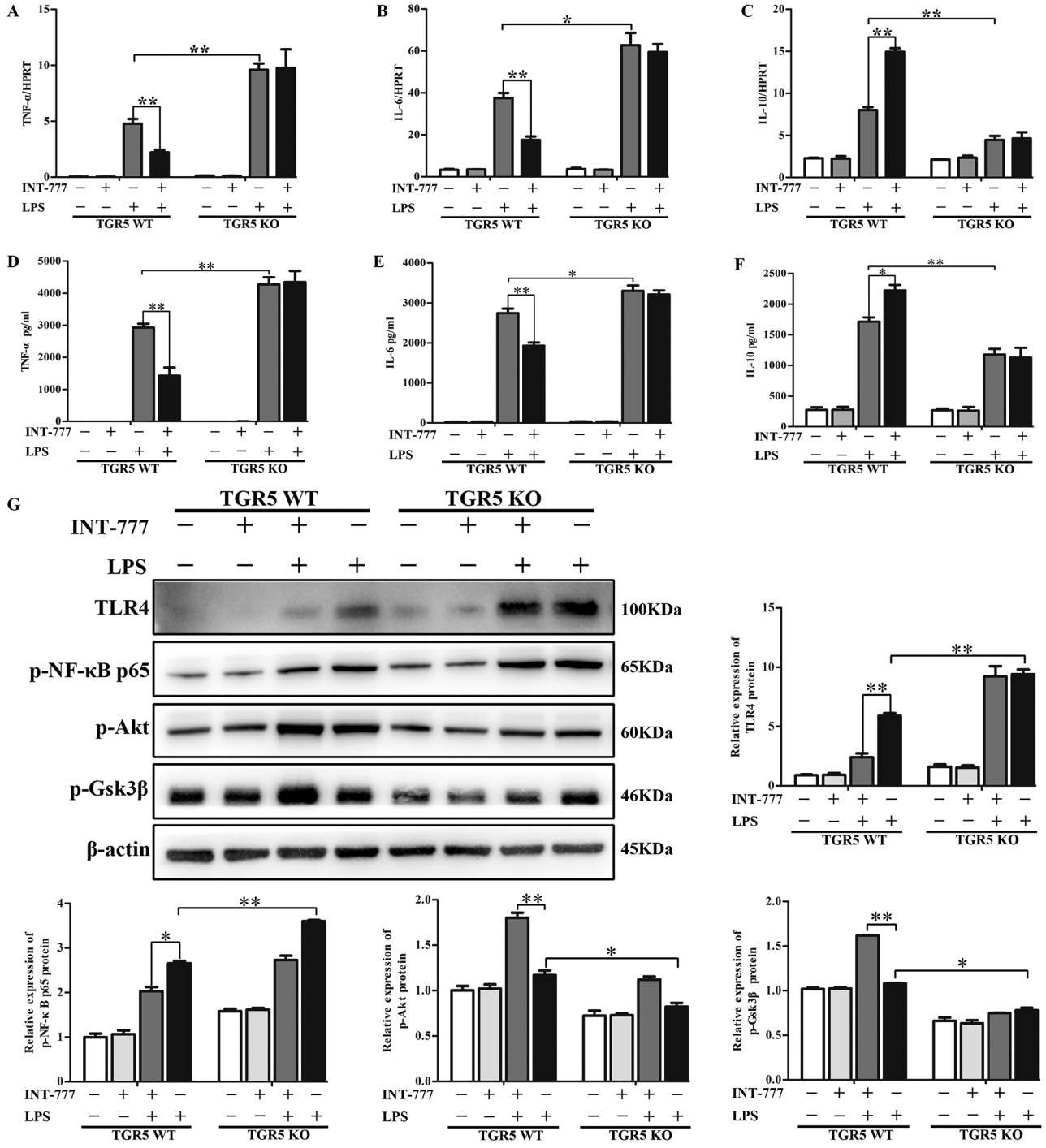

Fig. 4. TGR5 activation inhibited TLR4-mediated pro-inflammatory responses in macrophages. BMDMs were isolated from TGR5-proficient and TGR5-deficient mice, cultured and differentiated for 7 days, and then stimulated with LPS for 24 h. INT-777 was added 1 h before LPS stimulation. (A–C) TNF-α, IL-6 and IL-10 mRNA levels were measured with qRT-PCR (n = 4), and (D–F) serum cytokine levels were detected with ELISA (n = 4 for each group). (G) TLR4, p-NF-κB p65, p-Akt, p-Gsk3β and β-actin were detected by western blot (n = 3). Statistical analysis was performed by Student's t-test. Each column represented the mean ± SD. $^{*}P < 0.05$, $^{**}P < 0.01$.

with LPS (Fig. 6G). Notably, the absence of TGR5 significantly increased the number of macrophages able to migrate *in vitro* compared with WT BMDMs (Fig. 6H). Overall, these results indicated that the increase in macrophage recruitment and activation in liver tissue was due to TGR5 deficiency associated with enhanced chemokine expression and the fact that TGR5-deletion macrophages had a strong migratory capacity.

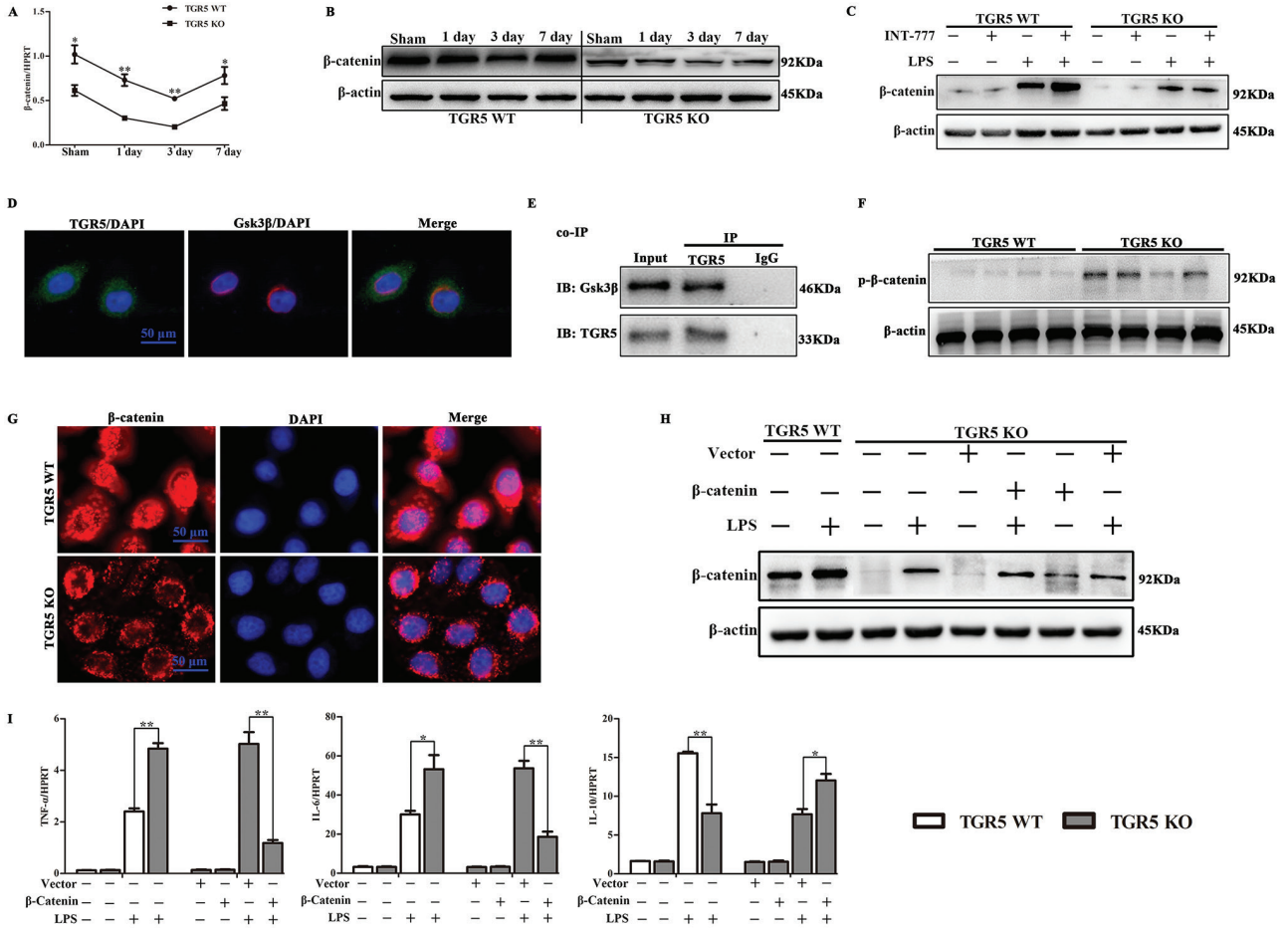

Fig. 5. β-catenin was essential for TGR5-mediated anti-inflammatory properties in macrophage. (A) qRT-PCR-assisted detection of β-catenin mRNA in WT and TGR5$^{-/-}$ mice at 1, 3 and 7 days after sham operation or BDL (n = 6 for each group). (B) Protein levels of β-catenin and β-actin in WT and TGR5$^{-/-}$ at 1, 3 and 7 days after sham operation or BDL, determined by western blot analysis (n = 3). (C) Western blot analysis of β-catenin in TGR5$^{-/-}$ and WT BMDMs pre-treated with INT-777, followed by LPS stimulation for 24 h (n = 3). (D) Co-localization of endogenous TGR5 and Gsk3β in macrophages was examined by confocal microscopy (n = 3 for each group). Scale bars: 50 μm. (E) Interaction of endogenous TGR5 with Gsk3β was examined by co-immunoprecipitation assay in BMDMs (n = 3). (F) p-β-catenin protein levels were determined by western blotting in WT and TGR5$^{-/-}$ BMDMs (n = 3). (G) The effect of TGR5 on active-β-catenin was analyzed by immunofluorescence staining using anti-active-β-catenin antibody (red) and DAPI nuclear staining (blue) (n = 3 for each group). Scale bars: 50 μm. TGR5$^{-/-}$ BMDMs were transfected with a lentivirus vector over-expressing β-catenin or control vector, followed by LPS stimulation. (H) β-catenin protein expression levels were measured by western blot (n = 3). (I) qRT-PCR-assisted detection of TNF-α, IL-6 and IL-10 mRNAs (n = 4). Statistical analysis was performed by Student's t-test. Each column represented the mean ± SD. *P < 0.05, **P < 0.01.

Administration of TGR5-deficient BMDMs aggravated BDL-induced CHI via modulating β-catenin signaling

WT C57BL/6 mice were irradiated at 5 Gy to destroy the bone marrow and were then subjected to BDL. BMDMs isolated from WT and TGR5$^{-/-}$ mice were cultured and differentiated for 7 days. TGR5$^{-/-}$ BMDMs differentiated under L929 conditions were transfected with the β-catenin-over-expressing or control vector, and 5 × 10^6 cells were injected into the tail veins of the irradiated mice, followed by BDL at 1 h after injection. Untreated BDL-induced CHI immune-deficiency mice were used as controls. Livers and serum were harvested at 3 days after BDL (Fig. 7A). The migration of donor BMDMs into liver was confirmed by tissue section staining. No statistical difference was observed in the number of BMDMs colonized in the liver of the above groups (Fig. 7B). sTBA, sTBIL, sALT, and sAST levels were all significantly increased in the WT BMDM-injection group compared with the untreated BDL group (Fig. 7C). BDL-induced CHI was more severe in mice injected with TGR5$^{-/-}$ BMDMs compared with the WT BMDM-injection group, while injection of TGR5$^{-/-}$ BMDMs overexpressing β-catenin markedly alleviated BDL-induced CHI. Moreover, TNF-α and IL-6 levels were significantly reduced and IL-10 protein expression levels in serum were significantly enhanced in mice administered WT BMDMs compared with the TGR5$^{-/-}$ BMDM-injection group, whereas the restoration of β-catenin expression in TGR5$^{-/-}$ BMDMs reduced the expression levels of TNF-α and IL-6, and enhanced IL-10 protein expression levels in serum compared with the TGR5$^{-/-}$ BMDM-injection group (Fig. 7D). Mice administered TGR5$^{-/-}$ BMDMs revealed significant liver edema, severe sinusoidal congestion/cytoplasmic vacuolization and extensive necrosis, whereas injection of TGR5$^{-/-}$ BMDMs

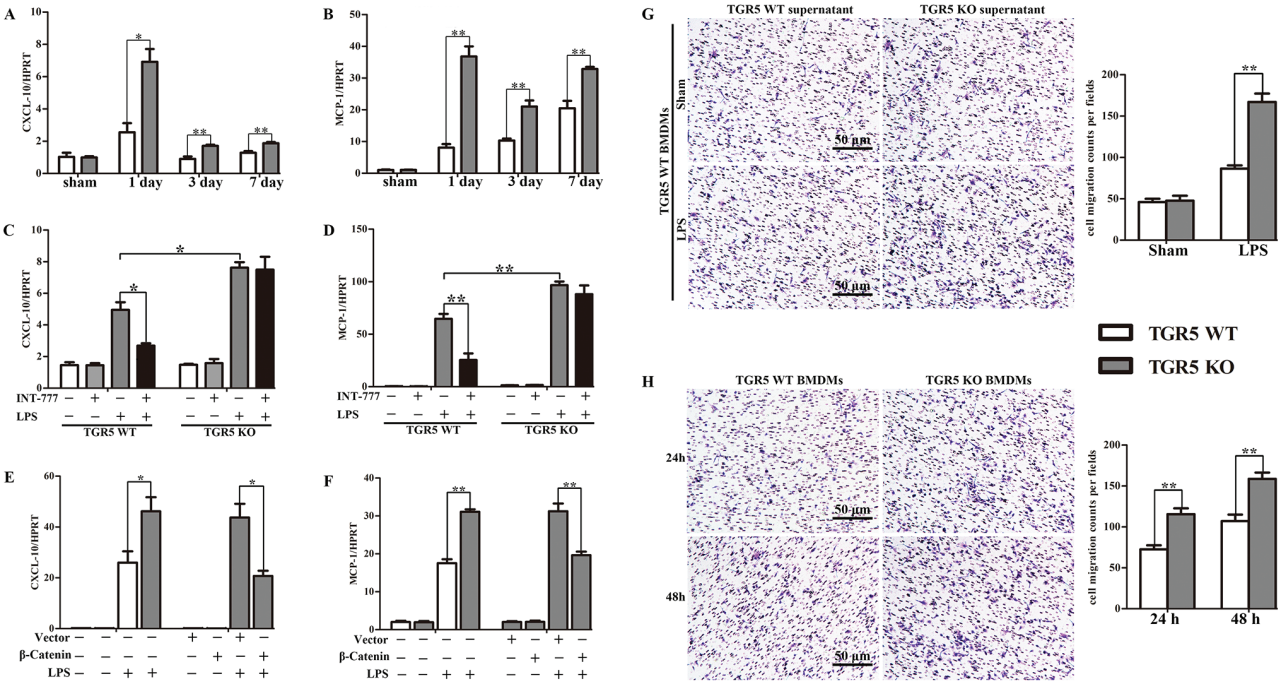

Fig. 6. TGR5 deletion induced chemokine expression and accelerated macrophage migration. (A and B) qRT-PCR-assisted detection of CXCL-10 and MCP-1 mRNA levels in TGR5-proficient and TGR5-deficient mice at 1, 3 and 7 days after sham operation or BDL ($n = 6$ for each group). WT and TGR5$^{-/-}$ BMDMs differentiated under L929 conditions were pre-treated with INT-777, followed by LPS stimulation for 24 h. (C and D) qRT-PCR-assisted detection of CXCL-10 and MCP-1 mRNA expression level ($n = 4$). TGR5$^{-/-}$ BMDMs were transfected with a lentivirus vector over-expressing β-catenin or control vector, followed by LPS stimulation. (E and F) qRT-PCR-assisted detection of CXCL-10 and MCP-1 mRNAs ($n = 4$). (G) Migration of WT macrophages in a transwell migration assay in response to supernatants from LPS-stimulated WT and TGR5$^{-/-}$ BMDMs ($n = 3$). Cell migration capability was quantified as cell numbers. (H) Macrophages isolated from WT and TGR5$^{-/-}$ mice migrated into transwell chamber pores ($n = 3$). Statistical analysis was performed by Student's *t*-test. The data were displayed as mean ± SD. $^{*}P < 0.05$, $^{**}P < 0.01$.

over-expressing β-catenin could partly rescue this effect (Fig. 7E).

Discussion

Bile duct obstruction plays a critical role in the progression of cholestatic liver disease, but the pathological mechanisms remain incompletely understood. The current study identified a novel mechanism underlying cholestatic liver disease using BDL-induced CHI. In this study, we demonstrated the following: (i) TGR5 played a crucial role in the control of local liver inflammation in immune-mediated CHI through activation of β-catenin signaling; (ii) TGR5 acted as a novel regulator of the β-catenin destruction complex by interacting with Gsk3β; (iii) TGR5-mediated β-catenin signaling also activated PI3K/Akt, inhibited the TLR4/NF-κB pathway, and attenuated the inflammatory responses.

GPCRs regulate cell migration, proliferation, differentiation and survival, and play a major role in the development and progression of many diseases, including inflammatory diseases and cancer (34–36). Many GPCRs induce NF-κB activation (37), but few inhibit NF-κB-mediated inflammation (14, 38). TGR5 was the first transmembrane GPCR shown to be activated by BAs, with DCA and LCA and their taurine and glycine conjugates functioning as physiological ligands (4, 5). In the immune system, TGR5 is primarily expressed by cells of myeloid origin, while T and B cells express the receptor at very low levels. TGR5 activation counteracts CD14/TLR4 activity in macrophages derived from peripheral blood and in liver macrophages, decreasing their phagocytic capacity and the production of the pro-inflammatory cytokines TNF-α, IL-1α and IL-6 (7, 39). TGR5 activation has previously been shown to inhibit LPS-induced expression of cytokines (14, 40). A previous study showed that TGR5 exerted anti-inflammatory effects, protected cholangiocytes from BA-induced toxicity, promoted cholangiocyte secretion and proliferation and reduced portal perfusion pressure (41). Stimulation of TGR5 signaling can improve steatohepatitis, portal hypertension and hepatic inflammation in rodent models of liver damage (42). Pean *et al.* demonstrated that TGR5 was crucial for liver protection against BA overload after partial hepatectomy, primarily through the control of bile hydrophobicity and cytokine secretion (43). However, the role of TGR5 in the chronic inflammatory response in CHI has not yet been reported. In the present study, we observed that TGR5 deficiency markedly aggravated BDL-induced liver injury, the inflammatory response and hepatic fibrosis. TGR5$^{-/-}$ macrophages were more susceptible to LPS stimulation than WT macrophages, and TGR5 activation by its ligand suppressed LPS-induced pro-inflammatory gene expression in WT but not TGR5$^{-/-}$ BMDMs. CXCL-10 is a chemokine that plays a role in the immune pathogenesis of inflammatory diseases, such as rheumatoid arthritis (44) and periodontal disease (45). CXCL-10 binds to its receptor, CXC chemokine receptor 3, and regulates immune responses by

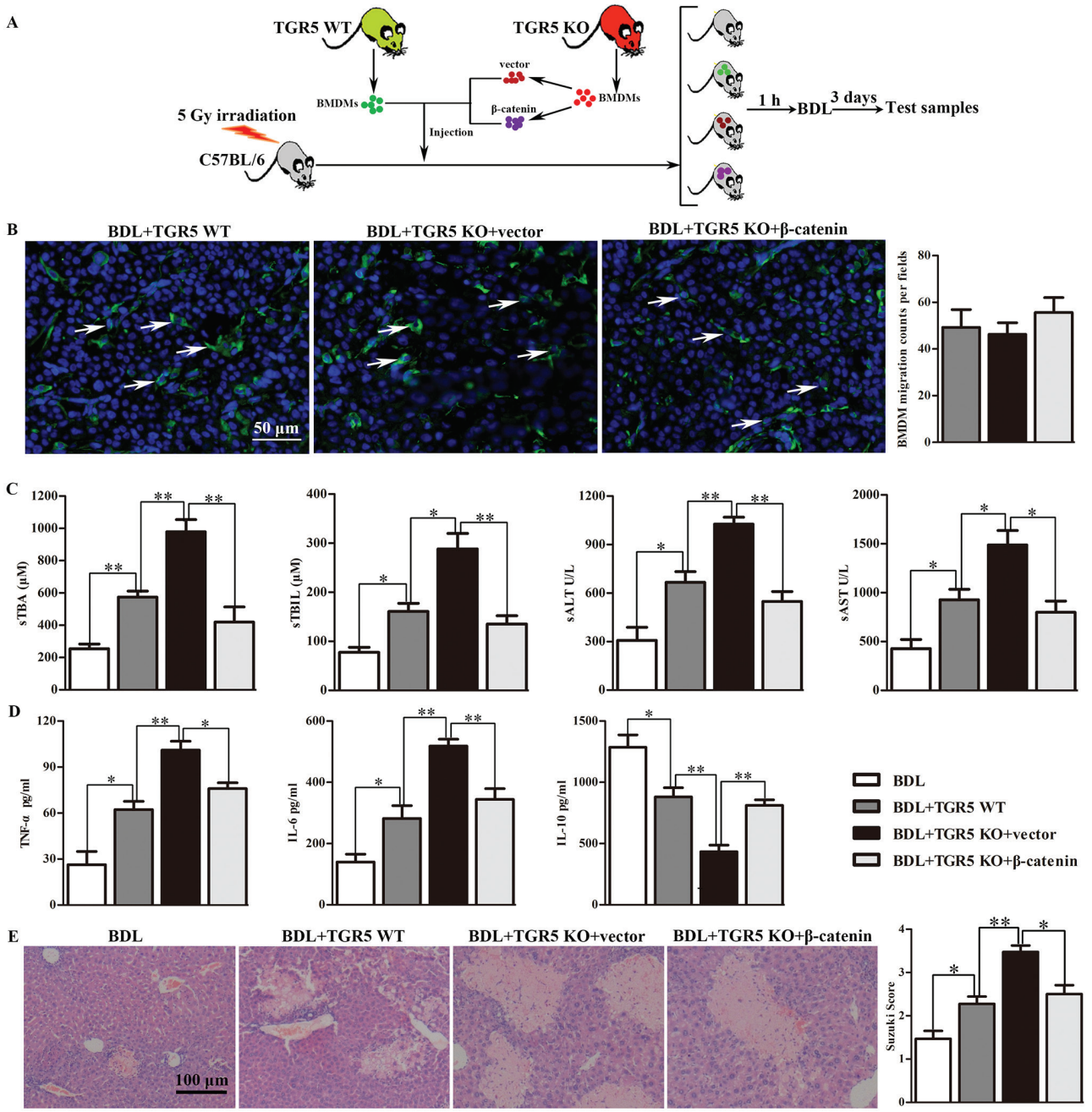

Fig. 7. Administration of TGR5-deficient BMDMs aggravated BDL-induced CHI via modulating β-catenin signaling. (A) BMDMs isolated from WT and TGR5$^{-/-}$ mice were cultured and differentiated for 7 days. TGR5$^{-/-}$ BMDMs differentiated under L929 conditions were transfected with β-catenin–over-expressing or control vector, and 5 × 10^6 cells were injected into the tail veins of irradiated mice. Bone marrow-irradiated C57BL/6 mice were subjected to BDL at 1 h after injection. Untreated BDL-induced CHI immune-deficient mice were used as controls. Mice were sacrificed at 3 days after BDL. (B) The cell membrane of each group of cells was labeled with PKH67 *in vitro*, and then cells were injected from the tail vein. The migration of injected macrophages into liver of the recipient mice was determined by tissue section staining (white arrows, scale bars: 50 μm). (C) Hepatocellular function was evaluated by sTBA, sTBIL, sALT and sAST (n = 6 for each group). (D) Protein levels of TNF-α, IL-6 and IL-10 in serum measured by ELISA (n = 6). (E) Histopathologic analysis of livers harvested 3 days after BDL (n = 5), and severity of liver injury according to Suzuki's histological grading. Scale bars: 100 μm. Statistical analysis was performed by Student's t-test. The data were displayed as mean ± SD. *P < 0.05, **P < 0.01.

activating and recruiting immune cells. MCP-1, also known as CCL2, was also shown to increase the macrophage content via proliferation of adipose tissue macrophages, in addition to its effect on blood monocyte recruitment (46). We demonstrated that CXCL-10 and MCP-1 expression levels were increased in TGR5$^{-/-}$ compared with WT cholestatic liver. This could be partially explained by the higher number of macrophages in this tissue, together with a direct effect of TGR5 activation on

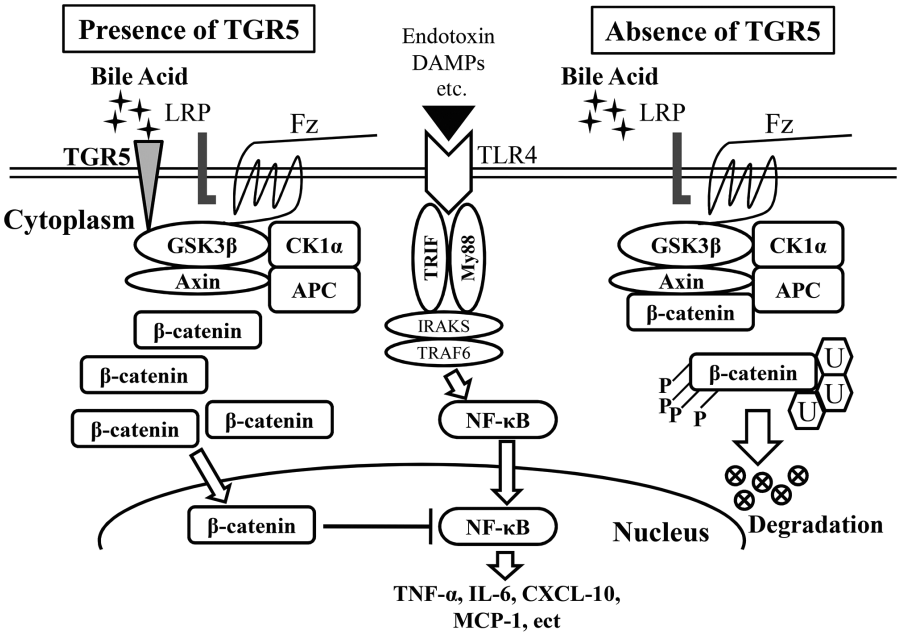

Fig. 8. Schematic of the proposed molecular mechanism whereby the TGR5/β-catenin axis regulates innate immune responses in BDL-induced liver inflammation.

CXCL-10 and MCP-1 in primary macrophages. Furthermore, TGR5-deficient macrophages have greater migration abilities than TGR5-proficient macrophages. We therefore propose that the reduced expression of CXCL-10 and MCP-1 subsequent to TGR5 activation may attenuate macrophage accumulation and alleviate CHI.

Regarding the molecular mechanisms underlying the anti-inflammatory function of TGR5 in cholestatic liver disease, a previous study reported that β-catenin signaling was required for control of innate and adaptive immunity during the inflammatory response (28). Activation of β-catenin in macrophages decreased pro-inflammatory cytokines and increased anti-inflammatory mediators (47). We therefore evaluated its influence on the Wnt/β-catenin signaling pathway, and showed that β-catenin was involved in the anti-inflammatory effect of TGR5, and β-catenin expression was effectively inhibited by TGR5 deficiency. The recent study found that TLR4/NF-κB/NLRP3 was significantly activated in cholestatic liver injury induced by bile duct ligation, which aggravated liver function damage, destruction of liver tissue structure and infiltration of inflammatory cells. Methane-rich saline treatment suppressed the TLR4/NF-κB pathway and further reduced the levels of pro-inflammatory factors during CHI (48). Previous studies investigated the regulatory relationship among the Wnt/β-catenin pathway and LPS-induced inflammation. For example, Jang *et al.* (49) reported that two Wnt inhibitors, Dickkopf-1 (DKK1) and LGK974, suppressed the LPS-induced inflammatory response by modulating the Wnt/β-catenin pathway. Li *et al.* (50) demonstrated that bone marrow mesenchymal stem cells protected alveolar macrophages from LPS-induced apoptosis, partially by inhibiting the Wnt/β-catenin pathway. β-catenin is also known to have a negative regulatory effect on the activity of NF-κB through direct interaction (51). However, the absence of β-catenin in hepatocytes and cholangiocytes conferred protection after BDL, characterized by a reduced BA pool, bile infarcts, fibrosis and inflammation (52). This may be explained by the fact that β-catenin expression exerts different functions in different kinds of liver cells to maintain immune homeostasis.

Gsk3β, as a major component of the cytoplasmic β-catenin destruction complex, modulated the phosphorylation and degradation of β-catenin. We therefore examined the relationship between TGR5 and Gsk3β. We demonstrated that macrophage TGR5 positively regulated β-catenin through direct binding to Gsk3β, disrupted the β-catenin destruction complex, and eventually promoted β-catenin signaling. Indeed, β-catenin expression was effectively repressed by TGR5 deficiency *in vivo*, while the pro-inflammatory functions of TGR5-knockout were almost abolished by transfection of BMDMs with a β-catenin-over-expressing lentivirus. There were no obvious correlations between TGR5 and other components of the β-catenin destruction complex (Axin, APC and CK1α) (data not shown).

In conclusion, we demonstrated that TGR5 regulates innate immune responses and macrophage migration in BDL-induced CHI. TGR5 directly interacts with Gsk3β, and subsequently disrupts the β-catenin destruction complex, thus activating β-catenin signaling, which in turn promotes PI3K/Akt signaling and inhibits the TLR4 pathway in cholestatic liver (Fig. 8). By identifying the molecular pathways whereby TGR5 regulates β-catenin-mediated innate immunity, our findings provide the rationale for novel therapeutic approaches to attenuate BDL-induced liver inflammation and injury.

Funding

This study was supported by the Foundation of Jiangsu Collaborative Innovation Center of Biomedical Functional Materials, the Priority Academic Program Development of Jiangsu Higher Education Institutions, the National Natural Science Foundation of China

(81871259, 81530048, 81400650, 814700901, 81273261, and 81270583), and Six Talent Peaks Project in Jiangsu Province (WSW-019).

Ethics statement

All animals received humane care and all animal procedures met the relevant legal and ethical requirements according to a protocol approved by the Institutional Animal Care and Use Committee of Nanjing Medical University.

Author contributions

X.W. and F.C. conceived and designed the experiments. J.R., C.Y., S.Y. and H.L. performed the experiments. J.R., Y.H., L.L. and F.C. analyzed the data. J.R. and C.Y. wrote the article.

Conflicts of interest statement: All authors declare no conflict of interests.

References

1 Liu, R., Zhao, R., Zhou, X. *et al.* 2014. Conjugated bile acids promote cholangiocarcinoma cell invasive growth through activation of sphingosine 1-phosphate receptor 2. *Hepatology* 60:908.
2 Hylemon, P. B., Zhou, H., Pandak, W. M., Ren, S., Gil, G. and Dent, P. 2009. Bile acids as regulatory molecules. *J. Lipid Res.* 50:1509.
3 Heymann, F. and Tacke, F. 2016. Immunology in the liver—from homeostasis to disease. *Nat. Rev. Gastroenterol. Hepatol.* 13:88.
4 Maruyama, T., Miyamoto, Y., Nakamura, T. *et al.* 2002. Identification of membrane-type receptor for bile acids (M-BAR). *Biochem. Biophys. Res. Commun.* 298:714.
5 Kawamata, Y., Fujii, R., Hosoya, M. *et al.* 2003. A G protein-coupled receptor responsive to bile acids. *J. Biol. Chem.* 278:9435.
6 Drucker, D. J. 2003. Enhancing incretin action for the treatment of type 2 diabetes. *Diabetes Care* 26:2929.
7 Watanabe, M., Houten, S. M., Mataki, C. *et al.* 2006. Bile acids induce energy expenditure by promoting intracellular thyroid hormone activation. *Nature* 439:484.
8 Thomas, C., Gioiello, A., Noriega, L. *et al.* 2009. TGR5-mediated bile acid sensing controls glucose homeostasis. *Cell Metab.* 10:167.
9 Maruyama, T., Tanaka, K., Suzuki, J. *et al.* 2006. Targeted disruption of G protein-coupled bile acid receptor 1 (Gpbar1/M-Bar) in mice. *J. Endocrinol.* 191:197.
10 Keitel, V., Donner, M., Winandy, S., Kubitz, R. and Haussinger, D. 2008. Expression and function of the bile acid receptor TGR5 in Kupffer cells. *Biochem. Biophys. Res. Commun.* 372:78.
11 Haselow, K., Bode, J. G., Wammers, M. *et al.* 2013. Bile acids PKA-dependently induce a switch of the IL-10/IL-12 ratio and reduce proinflammatory capability of human macrophages. *J. Leukoc. Biol.* 94:1253.
12 Perino, A., Pols, T. W., Nomura, M. *et al.* 2014. TGR5 reduces macrophage migration through mTOR-induced C/EBPbeta differential translation. *J. Clin. Invest.* 124:5424.
13 Pols, T. W., Nomura, M., Harach, T. *et al.* 2011. TGR5 activation inhibits atherosclerosis by reducing macrophage inflammation and lipid loading. *Cell Metab.* 14:747.
14 Wang, Y. D., Chen, W. D., Yu, D, Forman, B. M. and Huang, W. 2011. The G-protein-coupled bile acid receptor, Gpbar1 (TGR5), negatively regulates hepatic inflammatory response through antagonizing nuclear factor kappa light-chain enhancer of activated B cells (NF-kappaB) in mice. *Hepatology* 54:1421.
15 Monga, S. P. 2011. Role of Wnt/beta-catenin signaling in liver metabolism and cancer. *Int. J. Biochem. Cell Biol.* 43:1021.
16 Kimelman, D. and Xu, W. 2006. Beta-catenin destruction complex: insights and questions from a structural perspective. *Oncogene* 25:7482.
17 Sun, J., Hobert, M. E., Duan, Y. *et al.* 2005. Crosstalk between NF-kappaB and beta-catenin pathways in bacterial-colonized intestinal epithelial cells. *Am. J. Physiol. Gastrointest. Liver Physiol.* 289:G129.
18 Deng, J., Miller, S. A., Wang, H. Y., *et al.* 2002. Beta-catenin interacts with and inhibits NF-kappa B in human colon and breast cancer. *Cancer. Cell* 2:323.
19 Du, Q., Zhang, X., Cardinal, J. *et al.* 2009. Wnt/beta-catenin signaling regulates cytokine-induced human inducible nitric oxide synthase expression by inhibiting nuclear factor-kappaB activation in cancer cells. *Cancer. Res.* 69:3764.
20 Oya, S., Yokoyama, Y., Kokuryo, T. *et al.* 2014. Inhibition of Toll-like receptor 4 suppresses liver injury induced by biliary obstruction and subsequent intraportal lipopolysaccharide injection. *Am. J. Physiol. Gastrointest. Liver Physiol.* 306:G244.
21 Zhang, S., Wang, Z., Zhu, J. *et al.* 2018. Carnosic acid alleviates bdl-induced liver fibrosis through miR-29b-3p-mediated inhibition of the high-mobility group box 1/Toll-Like Receptor 4 signaling pathway in rats. *Front. Pharmacol.* 8:976.
22 Weng, Z., Chi, Y., Xie, J. *et al.* 2018. Anti-inflammatory activity of dehydroandrographolide by TLR4/NF-kappaB signaling pathway inhibition in bile duct-ligated mice. *Cell Physiol. Biochem.* 49:1083.
23 Neumann, J., Schaale, K., Farhat, K. *et al.* 2010. Frizzled1 is a marker of inflammatory macrophages, and its ligand Wnt3a is involved in reprogramming Mycobacterium tuberculosis-infected macrophages. *FASEB J.* 24:4599.
24 Lee, H., Bae, S., Choi, B. W. and Yoon, Y. 2012. WNT/beta-catenin pathway is modulated in asthma patients and LPS-stimulated RAW264.7 macrophage cell line. *Immunopharmacol. Immunotoxicol.* 34:56.
25 Malhotra, S. and Kincade, P. W. 2009. Canonical Wnt pathway signaling suppresses VCAM-1 expression by marrow stromal and hematopoietic cells. *Exp. Hematol.* 37:19.
26 Pereira, C. P., Bachli, E. B. and Schoedon, G. 2009. The wnt pathway: a macrophage effector molecule that triggers inflammation. *Curr. Atheroscler. Rep.* 11:236.
27 George, S. J. 2008. Wnt pathway: a new role in regulation of inflammation. *Arterioscler. Thromb. Vasc. Biol.* 28:400.
28 Ke, B, Shen, X. D., Kamo, N. *et al.* 2013. Beta-catenin regulates innate and adaptive immunity in mouse liver ischemia-reperfusion injury. *Hepatology* 57:1203.
29 Yang, H., Zhou, H., Zhuang, L. *et al.* 2017. Plasma membrane-bound G protein-coupled bile acid receptor attenuates liver ischemia/reperfusion injury via the inhibition of toll-like receptor 4 signaling in mice. *Liver Transpl.* 23:63.
30 Asgharpour, A., Kumar, D. and Sanyal, A. 2015. Bile acids: emerging role in management of liver diseases. *Hepatol. Int.* 9:527.
31 Kusumbe, A. P., Mali, A. M. and Bapat, S. A. 2009. CD133-expressing stem cells associated with ovarian metastases establish an endothelial hierarchy and contribute to tumor vasculature. *Stem Cells* 27:498.
32 McMahan, R. S., Birkland, T. P., Smigiel, K. S. *et al.* 2016. Stromelysin-2 (MMP10) moderates inflammation by controlling macrophage activation. *J. Immunol.* 197:899.
33 Jin, Y., Li, C., Xu, D. *et al.* 2019. Jagged1-mediated myeloid Notch1 signaling activates HSF1/Snail and controls NLRP3 inflammasome activation in liver inflammatory injury. *Cell. Mol. Immunol. doi:10.1038/s41423-019-0318-x*
34 Guo, C., Su, J., Li, Z. *et al.* 2015. The G-protein-coupled bile acid receptor Gpbar1 (TGR5) suppresses gastric cancer cell proliferation and migration through antagonizing STAT3 signaling pathway. *Oncotarget* 6:34402.
35 Han, L. Y., Fan, Y. C., Mu, N. N. *et al.* 2014. Aberrant DNA methylation of G-protein-coupled bile acid receptor Gpbar1 (TGR5) is a potential biomarker for hepatitis B Virus associated hepatocellular carcinoma. *Int. J. Med. Sci.* 11:164.
36 Casaburi, I., Avena, P., Lanzino, M. *et al.* 2012. Chenodeoxycholic acid through a TGR5-dependent CREB signaling activation enhances cyclin D1 expression and promotes human endometrial cancer cell proliferation. *Cell Cycle* 11:2699.

37 Fraser, C. C. 2008. G protein-coupled receptor connectivity to NF-kappaB in inflammation and cancer. *Int. Rev. Immunol.* 27:320.
38 Mediero, A., Perez-Aso, M. and Cronstein, B. N. 2013. Activation of adenosine A(2A) receptor reduces osteoclast formation via PKA- and ERK1/2-mediated suppression of NFkappaB nuclear translocation. *Br. J. Pharmacol.* 169:1372.
39 Newton, K. and Dixit, V. M. 2012. Signaling in innate immunity and inflammation. *Cold Spring Harb. Perspect. Biol.* 4:a006049.
40 Hogenauer, K., Arista, L., Schmiedeberg, N. *et al.* 2014. G-protein-coupled bile acid receptor 1 (GPBAR1, TGR5) agonists reduce the production of proinflammatory cytokines and stabilize the alternative macrophage phenotype. *J. Med. Chem.* 57:10343.
41 Reich, M., Deutschmann, K., Sommerfeld, A. *et al.* 2016. TGR5 is essential for bile acid-dependent cholangiocyte proliferation in vivo and in vitro. *Gut* 65:487.
42 Donepudi, A. C., Boehme, S., Li, F. and Chiang, J. Y. 2017.G-protein-coupled bile acid receptor plays a key role in bile acid metabolism and fasting-induced hepatic steatosis in mice. *Hepatology* 65:813.
43 Pean, N., Doignon, I., Garcin, I. *et al.* 2013. The receptor TGR5 protects the liver from bile acid overload during liver regeneration in mice. *Hepatology* 58:1451.
44 Lee, E. Y., Lee, Z. H. and Song, Y. W. 2013. The interaction between CXCL10 and cytokines in chronic inflammatory arthritis. *Autoimmun. Rev.* 12:554.
45 Garlet, G. P., Martins, W., Jr, Ferreira, B. R., Milanezi, C. M. and Silva, J. S. 2003. Patterns of chemokines and chemokine receptors expression in different forms of human periodontal disease. *J. Periodontal. Res.* 38:210.
46 Amano, S. U., Cohen, J. L., Vangala, P. *et al.* 2014. Local proliferation of macrophages contributes to obesity-associated adipose tissue inflammation. *Cell Metab.* 19:162.
47 Yue, S., Zhu, J., Zhang, M. *et al.* 2016. The myeloid heat shock transcription factor 1/beta-catenin axis regulates NLR family, pyrin domain-containing 3 inflammasome activation in mouse liver ischemia/reperfusion injury. *Hepatology* 64:1683.
48 Li, Z., Chen, D., Jia, Y. *et al.* 2019. Methane-rich saline counteracts cholestasis-induced liver damage via regulating the TLR4/NF-kappaB/NLRP3 inflammasome pathway. *Oxid. Med. Cell. Longev.* 2019:6565283.
49 Jang, J., Jung, Y., Kim, Y., Jho, E. H. and Yoon, Y. 2017. LPS-induced inflammatory response is suppressed by Wnt inhibitors, Dickkopf-1 and LGK974. *Sci. Rep.* 7:41612.
50 Li, B., Zhang, H., Zeng, M. *et al.* 2015. Bone marrow mesenchymal stem cells protect alveolar macrophages from lipopolysaccharide-induced apoptosis partially by inhibiting the Wnt/beta-catenin pathway. *Cell Biol. Int.* 39:192.
51 Nejak-Bowen, K., Kikuchi, A. and Monga, S. P. 2013. Beta-catenin-NF-kappaB interactions in murine hepatocytes: a complex to die for. *Hepatology* 57:763.
52 Thompson, M. D., Moghe, A., Cornuet, P. *et al.* 2018. Beta-catenin regulation of farnesoid X receptor signaling and bile acid metabolism during murine cholestasis. *Hepatology* 67:955.